A fast method for solving both the time-dependent Schrödinger equation in angular coordinates and its associated "*m*-mixing" problem

Matthew G. Reuter,[a] Mark A. Ratner, and Tamar Seideman
Department of Chemistry, Northwestern University, Evanston, Illinois 60208-3113, USA

(Received 26 June 2009; accepted 8 August 2009; published online 3 September 2009)

An efficient split-operator technique for solving the time-dependent Schrödinger equation in an angular coordinate system is presented, where a fast spherical harmonics transform accelerates the conversions between angle and angular momentum representations. Unlike previous techniques, this method features facile inclusion of azimuthal asymmetries (solving the "*m*-mixing" problem), adaptive time stepping, and favorable scaling, while simultaneously avoiding the need for both kinetic and potential energy matrix elements. Several examples are presented. © *2009 American Institute of Physics*. [doi:10.1063/1.3213436]

I. INTRODUCTION

The direct, numerical integration of the time-dependent Schrödinger equation (TDSE),

$$i\hbar\frac{d}{dt}|\Psi(t)\rangle = \hat{\mathcal{H}}(t)|\Psi(t)\rangle = (\hat{\mathcal{T}} + \hat{\mathcal{V}}(t))|\Psi(t)\rangle,$$
$$|\Psi(t_0)\rangle = |\Psi_0\rangle, \tag{1}$$

has become an essential component of molecular quantum dynamics. In such studies, the computational effort is spent propagating $|\Psi(t_0)\rangle$ to $|\Psi(t_0+\Delta t)\rangle$,

$$|\Psi(t_0+\Delta t)\rangle = \hat{\mathcal{U}}(t_0,\Delta t)|\Psi(t_0)\rangle, \tag{2}$$

where the propagator $\hat{\mathcal{U}}$ is generally not known or is computationally expensive due to the noncommutivity of the kinetic energy $\hat{\mathcal{T}}$ and the potential energy $\hat{\mathcal{V}}(t)$. One thus resorts to approximations of $\hat{\mathcal{U}}$ (Refs. 1 and 2) which balance several properties including unitarity, computational efficiency, the use of kinetic and potential energy matrix elements, and, although not critical, adaptive time stepping.

The second-order, split-operator propagator,

$$\hat{\mathcal{U}}(t_0,\Delta t) \approx e^{-i\hat{\mathcal{T}}\Delta t/(2\hbar)}e^{-i\hat{\mathcal{V}}(t_0+\Delta t/2)\Delta t/\hbar}e^{-i\hat{\mathcal{T}}\Delta t/(2\hbar)}, \tag{3}$$

achieves unitarity, the obviation of matrix elements, and adaptive time stepping, provided Δt is sufficiently small.[3] Each factor is evaluated in its local representation—momentum space for $\hat{\mathcal{T}}$ and position space for $\hat{\mathcal{V}}(t_0+\Delta t/2)$—necessitating a change in representation between each factor. As such, these transformations become the computational bottlenecks for this propagator; they generally scale quadratically with the number of basis states, N. Furthermore, since these transformations depend on the choice of coordinate system (often related to $\hat{\mathcal{T}}$) and *not* on the specific physical system, the optimization of a particular transform (a coordinate-dependent fast transform) would make this propagator efficient for a broad class of problems. General methods for algebraically deriving fast transforms have been proposed.[4]

For instance, when Cartesian coordinates are used, the momentum eigenstates are the Fourier modes, and the fast Fourier transform (FFT) accelerates the change of representation.[5–7] In this case, the split-operator technique also becomes computationally efficient, scaling as $\mathcal{O}(N \log N)$.

Unfortunately, not all systems of interest are naturally described by Cartesian coordinates. For example, investigations of atomic systems, molecular bending, and molecular alignment all include at least one angular variable. In these systems, the normalized spherical harmonics,

$$\tilde{Y}_\ell^m(\theta,\varphi) = \sqrt{\frac{1}{2\pi}}\tilde{P}_\ell^m(\cos(\theta))e^{im\varphi}, \tag{4}$$

rather than the Fourier modes, are the angular momentum eigenstates, and the computational efficiency from the FFT is lost.[8] Here, $0 \leqslant \theta \leqslant \pi$ is the polar Euler angle, $0 \leqslant \varphi < 2\pi$ is the azimuthal angle, and $\tilde{P}_\ell^m(x)$ is the normalized associated Legendre function of degree ℓ and order m.

Angular variables also introduce two new computational problems. First, the kinetic energy operator includes $\csc(\theta)$ terms that trouble numerical schemes as θ tends to 0 or π. Second is the so-called "*m*-mixing" problem, which occurs when $\hat{\mathcal{V}}(t)$ couples states of differing m values [as is often the case when $\hat{\mathcal{V}}(t)$ lacks azimuthal symmetry]. Originating from the $|m|$-dependence of optimal Gauss–Jacobi quadrature rules, the *m*-mixing problem is numerical: the nonconservation of m introduces suboptimal accuracy in numerical integration and/or necessitates interpolation between $|m|$-dependent quadrature grids. Recent work has overcome the *m*-mixing problem for potentials expressible as finite sums of *m*-conserving potentials;[9] however, a general solution has proven elusive.

With these two new considerations in mind, several propagators have been suggested for solving the TDSE with angular variables.[8–11] Most of these techniques successfully

[a]Electronic mail: mgreuter@u.northwestern.edu.

handle the $\csc(\theta)$ terms and are unitary, but compromise between the use of matrix elements, computational efficiency, and adaptive time stepping. As implied, none solve the m-mixing problem in full generality.

The development of a fast spherical harmonics transform[12] (FSHT) in recent years holds great promise for solving the TDSE in an angular coordinate system. We first assume our wavefunction is band limited, that is, we can choose a positive integer $\ell_{\max}$, such that

$$\Psi(\theta,\varphi,t) = \sum_{\ell=0}^{\ell_{\max}-1} \sum_{m=-\ell}^{\ell} \Psi_\ell^m(t)\tilde{Y}_\ell^m(\theta,\varphi) = \sum_{m=-\ell_{\max}+1}^{\ell_{\max}-1} e^{im\varphi} \sum_{\ell=|m|}^{\ell_{\max}-1} \frac{\Psi_\ell^m(t)}{\sqrt{2\pi}} \tilde{P}_\ell^m(\cos(\theta)), \quad (5)$$

where

$$\Psi_\ell^m(t) = \langle \tilde{Y}_\ell^m | \Psi(t) \rangle = \int_0^{2\pi} d\varphi \int_0^{\pi} d\theta \sin(\theta) \Psi(\theta,\varphi,t) \times (\tilde{Y}_\ell^m(\theta,\varphi))^*.$$

Given a set of $\Psi_\ell^m(t)$ coefficients, the FSHT calculates $\Psi(\theta,\varphi,t)$ at specific $\{\theta_i,\varphi_j\}$ grid points in $\mathcal{O}(\ell_{\max}{}^2 \log \ell_{\max})$ time. The inverse operation (grid points to coefficients) scales similarly. For comparison to the Cartesian equivalent, we note that there are $N=\ell_{\max}{}^2$ basis states here, so the scaling is $\mathcal{O}(N \log N)$.

Returning to the split-operator propagator, the FSHT is the angular analog of the Cartesian FFT as it accelerates the likewise transformation between angle and angular momentum representations [Eq. (5)]. The method presented in this work employs the FSHT for such transformations, yielding a propagator [Eq. (3)] that (i) is unitary, (ii) handles the $\csc(\theta)$ terms indirectly through the spherical harmonics, (iii) scales well, (iv) obviates the need for both kinetic and potential energy matrix elements, (v) exhibits adaptive time stepping, and (vi) solves the m-mixing problem. The layout of this paper is as follows. Section II summarizes the FSHT algorithm from Ref. 12. Section III presents several examples of this propagator, highlighting its functionality under mixed m. Finally, Sec. IV draws several conclusions.

II. THE FSHT

Reference 12 presents a FSHT algorithm that efficiently computes the $\Psi_\ell^m(t)$ coefficients in Eq. (5) from the values of $\Psi(\theta,\varphi,t)$ at specific $\{\theta_i,\varphi_j\}$ grid points and vice versa. Here we present an overview of this algorithm, referring the reader to Ref. 12 and the references within it for additional details. Some of these references are duplicated here.

For convenience, we require $\ell_{\max}$ to be an even, positive integer. The grid uses θ_i from the $(2\ell_{\max})$th order Gauss–Legendre quadrature rule,

$$P_{\ell_{\max}}(\cos(\theta_i)) = 0, \quad (6)$$

$i=1,2,\ldots,\ell_{\max}$, where $P_\ell(x)$ is the Legendre polynomial of degree ℓ $(m=0)$. The φ_j are evenly distributed,

$$\varphi_j = 2\pi(j-1)/(2\ell_{\max}-1), \quad (7)$$

$j=1,2,\ldots,(2\ell_{\max}-1)$.

Much of the efficiency of the FSHT is obtained through the one-dimensional fast multipole method[13] (FMM) and an efficient algorithm for manipulating symmetric, tridiagonal matrices.[14] Briefly, the FMM is an approximate, although arbitrarily accurate, method to compute matrix-vector products of the form

$$v_j = \sum_k u_k K(x_k - y_j) \quad (8)$$

in linear time, as opposed to quadratic time needed for general matrix-vector products. Two kernels are needed for the FSHT: $K(x-y)=(x-y)^{-1}$ and $K(x-y)=(x-y)^{-2}$. The tridiagonal matrix algorithm utilizes the FMM to apply the eigenvector matrix (or its transpose) of a symmetric, tridiagonal $M\times M$ matrix to an arbitrary vector in $\mathcal{O}(M \log M)$ time. Finally, the FSHT requires an extensive amount of precomputations, which need only be performed once for each $\ell_{\max}$. Before discussing the FSHT algorithm, we outline the precomputations and introduce our notation.[15]

A. FSHT precomputations

As will be seen in the discussion of the FSHT algorithm, the FSHT works with linear combinations of exclusively odd or exclusively even associated Legendre functions without loss in generality. As such, we will use x and y as the independent variables for the even and odd cases, respectively $(0\leqslant x,y\leqslant 1)$. Note that $\theta=\arccos(x)$ or $\theta=\arccos(y)$ for use in angular coordinate systems.

For each $|m|=0,1,\ldots,(\ell_{\max}-1)$ we need the following data.

(1) The Gauss–Jacobi quadrature abscissas and weights from $\tilde{P}^{|m|}_{|m|+2n_x^{|m|}}(x)$ and $\tilde{P}^{|m|}_{|m|+2n_y^{|m|}+1}(y)$, where

$$n_x^{|m|} = \mathrm{ceil}((\ell_{\max}-|m|)/2)$$

is the number of roots of $\tilde{P}^{|m|}_{|m|+2n_x^{|m|}}(x)$ in (0, 1) and

$$n_y^{|m|} = \mathrm{floor}((\ell_{\max}-|m|)/2)$$

is similarly the number of roots of $\tilde{P}^{|m|}_{|m|+2n_y^{|m|}+1}(y)$ in (0, 1). We will denote the even quadrature rule as $\{x_i^{|m|},\rho_i^{|m|}\}$ $(i=1,2,\ldots,n_x^{|m|})$ and the odd quadrature rule as $\{y_j^{|m|},\sigma_j^{|m|}\}$ $(j=1,2,\ldots,n_y^{|m|})$,

$$0 = \tilde{P}^{|m|}_{|m|+2n_x^{|m|}}(x_i^{|m|}), \quad (9)$$

$$0 = \tilde{P}^{|m|}_{|m|+2n_y^{|m|}+1}(y_j^{|m|}), \quad (10)$$

and

$$\rho_i^{|m|} = \frac{(2|m|+4n_x^{|m|}+1)(1-(x_i^{|m|})^2)^{|m|-1}}{[(\tilde{P}^{|m|}_{|m|+2n_x^{|m|}})'(x_i^{|m|})]^2}, \quad (11)$$

$$\sigma_j^{|m|} = \frac{(2|m| + 4n_y^{|m|} + 3)(1 - (y_j^{|m|})^2)^{|m|-1}}{[(\tilde{P}^{|m|}_{|m|+2n_y^{|m|}+1})'(y_j^{|m|})]^2}. \quad (12)$$

Equations (11) and (12) use f' to denote the derivative of f. Furthermore, due to its relation to the FSHT θ grid points, the even quadrature rule for $m=0$ will be denoted $\{z_k, w_k\}$ $(k=1,2,\ldots,(\ell_{\max}/2))$. An efficient algorithm for the computation of these quadrature rules is presented in Ref. 16.

(2) Interpolation data for converting between quadrature grids: $\{\tilde{P}^{|m|}_{|m|+2n_x^{|m|}}(z_k)\}$, $\{\tilde{P}^{|m|}_{|m|+2n_x^{|m|}-2}(x_i^{|m|})\}$, $\{\tilde{P}^{|m|}_{|m|+2n_y^{|m|}+1}(z_k)\}$, and $\{\tilde{P}^{|m|}_{|m|+2n_y^{|m|}-1}(y_j^{|m|})\}$.

(3) Precomputations for the tridiagonal matrix algorithm. The even tridiagonal matrix $\mathbf{S}^{|m|}$ has diagonal $\{d^{|m|}_{|m|+2i}\}$ $(i=0,1,\ldots,(n_x^{|m|}-1))$, where

$$d_\ell^m = \frac{2\ell(\ell+1) - 2m^2 - 1}{(2\ell-1)(2\ell+3)}, \quad (13)$$

sub- (super-) diagonal $\{c^{|m|}_{|m|+2i}\}$ $(i=0,1,\ldots,(n_x^{|m|}-2))$,

$$c_\ell^m = \sqrt{\frac{(\ell-m+1)(\ell-m+2)(\ell+m+1)(\ell+m+2)}{(2\ell+1)(2\ell+3)^2(2\ell+5)}}, \quad (14)$$

and eigenvector matrix $\mathbf{U}^{|m|}$, such that $\mathbf{S}^{|m|} = \mathbf{U}^{|m|}\mathbf{\Lambda}^{|m|}(\mathbf{U}^{|m|})^T$. The corresponding odd tridiagonal matrix $\mathbf{T}^{|m|}$ has diagonal $\{d^{|m|}_{|m|+2i+1}\}$ $(i=0,1,\ldots,(n_y^{|m|}-1))$, sub- (super-) diagonal $\{c^{|m|}_{|m|+2i+1}\}$ $(i=0,1,\ldots,(n_y^{|m|}-2))$, and eigenvector matrix $\mathbf{V}^{|m|}$, such that $\mathbf{T}^{|m|} = \mathbf{V}^{|m|}\mathbf{\Gamma}^{|m|}(\mathbf{V}^{|m|})^T$. We note that $\mathbf{\Lambda}^{|m|}$ and $\mathbf{\Gamma}^{|m|}$ are diagonal matrices with elements related to $\{x_i^{|m|}\}$ and $\{y_j^{|m|}\}$, respectively.

(4) Normalization matrices,

$$(\mathbf{A}^{|m|})_{j,k} = \delta_{j,k}\sqrt{\sum_{i=0}^{n_x^{|m|}-1}(\tilde{P}^{|m|}_{|m|+2i}(x_j^{|m|}))^2} \quad (15)$$

and

$$(\mathbf{B}^{|m|})_{j,k} = \delta_{j,k}\sqrt{\sum_{i=0}^{n_y^{|m|}-1}(\tilde{P}^{|m|}_{|m|+2i+1}(y_j^{|m|}))^2}. \quad (16)$$

B. The FSHT algorithm

Figure 1 displays a schematic of the FSHT algorithm for converting angular grid data $\Psi(\theta,\varphi)$ into the coefficients of the spherical harmonics expansion, Ψ_ℓ^m. The inverse operation can be performed by backtracing the flowchart in Fig. 1.

The FSHT algorithm starts with the angular grid data, $\Psi(z_i,\varphi_j)$, where $-1<z_i=\cos(\theta_i)<1$ and the $\{\theta_i\}$ and $\{\varphi_j\}$ are given by Eqs. (6) and (7). The first step is to separate the even and odd components (with respect to z) of Ψ, denoted by χ and Φ, respectively. Accordingly,

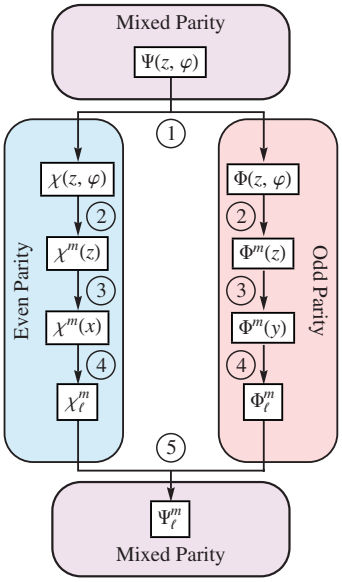

FIG. 1. Schematic outline of the FSHT algorithm. The procedure is reversed for the inverse operation. (1) Split the grid points into even and odd components with respect to $z=\cos(\theta)$. (2) Use the FFT over the azimuthal angle φ to obtain m populations. (3) Interpolate from the even, $m=0$ quadrature grid, $\{z_k\}$, to the appropriate quadrature grid. (4) Perform an associated Legendre transform over the polar angle θ. (5) Merge the separated even- and odd-parity data.

$$\chi(z_i,\varphi_j) = \frac{\Psi(z_i,\varphi_j) + \Psi(-z_i,\varphi_j)}{2} \quad (17)$$

and

$$\Phi(z_i,\varphi_j) = \frac{\Psi(z_i,\varphi_j) - \Psi(-z_i,\varphi_j)}{2}, \quad (18)$$

where $0<z_i<1$ for χ and Φ.

The second step utilizes the FFT over φ to determine populations in each m-level. A total of $\ell_{\max}$ FFTs are performed, one for each z_i value for both χ and Φ. This produces $\chi^m(z_i)$ and $\Phi^m(z_i)$, where $m=-(\ell_{\max}-1),\ldots,0,\ldots,(\ell_{\max}-1)$.

The third step interpolates the functions from the $\{z_i\}$ points to the $\{x_i^{|m|}\}$ or $\{y_i^{|m|}\}$ points, depending on parity. Results from the Christoffel–Darboux identities are used here, producing

$$\chi^m(x_j^{|m|}) = c^{|m|}_{|m|+2n_x^{|m|}-2}\tilde{P}^{|m|}_{|m|+2n_x^{|m|}-2}(x_j^{|m|}) \times \sum_{i=1}^{\ell_{\max}/2}\frac{2w_i\tilde{P}^{|m|}_{|m|+2n_x^{|m|}}(z_i)\chi^m(z_i)}{z_i^2-(x_j^{|m|})^2}, \quad (19)$$

$$\Phi^m(y_j^{|m|}) = c^{|m|}_{|m|+2n_x^{|m|}-1}\tilde{P}^{|m|}_{|m|+2n_x^{|m|}-1}(y_j^{|m|}) \times \sum_{i=1}^{\ell_{\max}/2}\frac{2w_i\tilde{P}^{|m|}_{|m|+2n_x^{|m|}+1}(z_i)\Phi^m(z_i)}{z_i^2-(y_j^{|m|})^2}. \quad (20)$$

While this interpolation generally scales quadratically, the FMM can be used to make it scale linearly. The reverse interpolation (needed for the inverse FSHT operation) can be performed using

$$\chi^m(z_i) = c^{|m|}_{|m|+2n_x^{|m|}-2}\tilde{P}^{|m|}_{|m|+2n_x^{|m|}}(z_i) \times \sum_{j=1}^{n_x^{|m|}} \frac{\hat{\rho}_j^{|m|}\tilde{P}^{|m|}_{|m|+2n_x^{|m|}-2}(x_j^{|m|})\chi^m(x_j^{|m|})}{z_i^2-(x_j^{|m|})^2}, \quad (21)$$

$$\Phi^m(z_i) = c^{|m|}_{|m|+2n_x^{|m|}-1}\tilde{P}^{|m|}_{|m|+2n_x^{|m|}+1}(z_i) \times \sum_{j=1}^{n_y^{|m|}} \frac{\hat{\sigma}_j^{|m|}\tilde{P}^{|m|}_{|m|+2n_x^{|m|}-1}(y_j^{|m|})\Phi^m(y_j^{|m|})}{z_i^2-(y_j^{|m|})^2}, \quad (22)$$

where

$$\hat{\rho}_j^{|m|} = 2\rho_j^{|m|}(1-(x_j^{|m|})^2)^{-|m|}, \quad (23)$$

$$\hat{\sigma}_j^{|m|} = 2\sigma_j^{|m|}(1-(y_j^{|m|})^2)^{-|m|}. \quad (24)$$

The fourth step transforms the remaining x or y grid to ℓ using an associated Legendre transform. If we define the vectors $\vec{\alpha}^m$ and $\vec{\mu}^m$ to have elements $\alpha_i^m=\chi^m(x_i^{|m|})$ and $\mu_j^m=\Phi^m(y_j^{|m|})$, the associated Legendre transform can be calculated by

$$\vec{\beta}^m = \mathbf{U}^{|m|}(\mathbf{A}^{|m|})^{-1}\vec{\alpha}^m, \quad (25)$$

$$\vec{\nu}^m = \mathbf{V}^{|m|}(\mathbf{B}^{|m|})^{-1}\vec{\mu}^m. \quad (26)$$

Here $\mathbf{A}^{|m|}$ and $\mathbf{B}^{|m|}$ are diagonal, and $\mathbf{U}^{|m|}$ and $\mathbf{V}^{|m|}$ are the eigenvector matrices of symmetric, tridiagonal matrices, allowing these matrix-vector products to be computed in subquadratic time. The coefficients χ_ℓ^m and Φ_ℓ^m can be obtained from $\vec{\beta}^m$ and $\vec{\nu}^m$, respectively. When $m\geqslant 0$, $\chi^m_{|m|+2i}=\beta^m_{i+1}$, and $\Phi^m_{|m|+2j+1}=\nu^m_{j+1}$ for $i=0,1,\ldots,(n_x^{|m|}-1)$ and $j=0,1,\ldots,(n_y^{|m|}-1)$. Since

$$\tilde{P}_\ell^{-|m|}(z) = (-1)^m\tilde{P}_\ell^{|m|}(z),$$

$\chi^m_{|m|+2i}=(-1)^m\beta^m_{i+1}$ and $\Phi^m_{|m|+2j+1}=(-1)^m\nu^m_{j+1}$ when $m<0$. The inverse operations,

$$\vec{\alpha}^m = \mathbf{A}^{|m|}(\mathbf{U}^{|m|})^T\vec{\beta}^m, \quad (27)$$

$$\vec{\mu}^m = \mathbf{B}^{|m|}(\mathbf{V}^{|m|})^T\vec{\nu}^m, \quad (28)$$

are similar and can also be computed quickly. The fifth and final step of the FSHT merges the odd and even expansion coefficients, which is an exercise in computer memory management.

III. EXAMPLES

The FSHT was implemented in C using the CVODE library[17] in the precomputations and the FFTW package[18] for the FFT. We now present two examples demonstrating how this split-operator propagator addresses the six properties outlined in Sec. I. We begin by noting that this FSHT-accelerated propagator, by construction, does not require kinetic and potential energy matrix elements. Furthermore, the original presentation of the FSHT algorithm[12] provides ample substantiation of its favorable scaling.

Our first example demonstates the propagator's unitarity[19] and its adequate management of the csc θ terms. Sets of Ψ_ℓ^m coefficients for numerous $\ell_{\max}\lesssim 1600$ were randomly generated, normalized, and subjected to the backward and forward FSHT operations 100 times. After the series of transformations, the average absolute error in each coefficient was $\sim 10^{-7}$ with a corresponding average relative error of $\sim 10^{-4}$. The small errors realized through numerous applications of the FSHT show that the propagator is unitary and is not troubled by the csc θ terms.

We proceed to show that the split-operator propagator with the FSHT is capable of adaptive time stepping and generally solves the m-mixing problem. For our second example, we consider the alignment of Cl_2 in response to a linearly polarized electric field. When the electric field is polarized along the z-axis, the field-induced potential is[20]

$$\hat{\mathcal{V}}_z(t) = -\varepsilon^2(t)\Delta\alpha\cos^2(\theta_z)/4, \quad (29)$$

where $\varepsilon(t)$ is the electric field amplitude, $\Delta\alpha$ is the polarizability anisotropy of the linear top molecule, and (θ_z,φ_z) are the polar and azimuthal angles in this coordinate system. A physical motivation (such as a second electromagnetic field or a surface) may instead orient the laser field along the x-axis, producing a potential

$$\hat{\mathcal{V}}_x(t) = -\varepsilon^2(t)\Delta\alpha\sin^2(\theta_x)\cos^2(\varphi_x)/4, \quad (30)$$

where (θ_x,φ_x) are the canonical angles in this second coordinate system.

The potential $\hat{\mathcal{V}}_z(t)$ is azimuthally symmetric and does not mix m states, whereas this symmetry is broken in $\hat{\mathcal{V}}_x(t)$, subjecting the simulation to the m-mixing problem. Since the physics is independent of the choice of coordinate system, use of the propagator from equivalent initial states should produce identical results. We choose the initial state to be the ground state,

$$\Psi_x(\theta_x,\varphi_x,0) = \tilde{Y}_0^0(\theta_x,\varphi_x),$$

$$\Psi_z(\theta_z,\varphi_z,0) = \tilde{Y}_0^0(\theta_z,\varphi_z),$$

and the electric field amplitude to be a Gaussian peaked at an intensity of 5×10^{13} W cm^{-2} with a standard deviation of 133 ps.

Figure 2(a) shows the degree of alignment, $\langle\cos^2\theta_z\rangle$, as a function of time. As expected, the degree of alignment increases from the isotropic value of $1/3$ as the field turns on and evolves back to the isotropic value as the field turns off. The degree of alignment is comparably $\langle\sin^2\theta_x\cos^2\varphi_x\rangle$ in the x-coordinate system, and the absolute error between the two degrees of alignment is displayed in Fig. 2(b). The numerically insignificant errors suggest that this propagator solves the m-mixing problem. To further substantiate this claim, Fig. 2(c) plots the populations in various m levels in the two coordinate systems. As expected, all population remains in $m_z=0$ for the z-coordinate system. In the m-mixed x-coordinate system, however, all population starts and ends in $m_x=0$, but transiently appears in other m_x-levels.

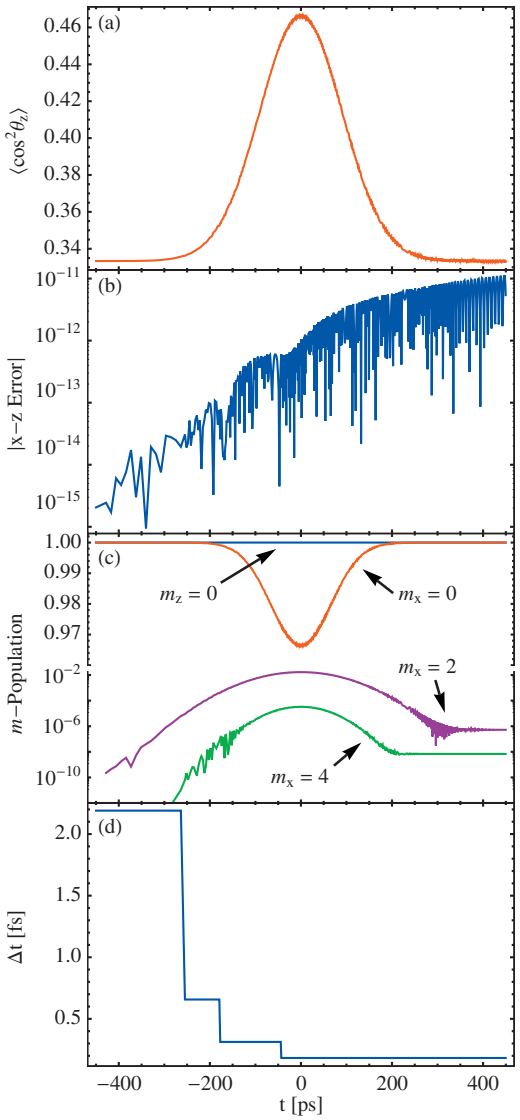

FIG. 2. Calculated solutions of the TDSE for the alignment of Cl_2. (a) The degree of alignment as a function of time for a Gaussian electric field amplitude with maximum intensity of 5×10^{13} W cm^{-2} and standard deviation of 133 ps. (b) The absolute error (in magnitude) in the degree of alignment between calculations in the two coordinate systems. The negligible error shows that this propagator is not affected by azimuthal asymmetries, solving the m-mixing problem. (c) Populations in various m levels for the two coordinate systems. All population remains in m_z=0 for the azimuthally symmetric potential, as expected. Without the azimuthal symmetry, population transfers between m_x levels are observed. (d) Demonstration of the adaptive time-stepping capability of the propagator. When only low-energy states are populated, larger time steps can be taken.

Finally, Fig. 2(d) shows the time step used during the propagation. The time step was chosen by satisfying

$$\max\left\{\left|\frac{\tilde{T}\Delta t}{\hbar}\right|,\left|\frac{\tilde{V}(t+\Delta t/2)\Delta t}{\hbar}\right|\right\}=\frac{\pi}{3}, \tag{31}$$

where $\tilde{T}$ is the largest eigenvalue (in magnitude) of $\hat{T}$ whose corresponding eigenstate has non-negligible population, and similarly for $\tilde{V}(t+\Delta t/2)$ and $\hat{\mathcal{V}}_{x,z}(t+\Delta t/2)$.

IV. CONCLUSIONS

Solutions to the TDSE in angular coordinates are important to a large variety of areas, ranging from atomic physics and molecular spectroscopy to chemical reactions and spintronics. Since the exact propagator is not easily obtainable, approximations that balance (i) unitarity, (ii) the use of kinetic and potential energy matrix elements, (iii) computational efficiency, (iv) adaptive time stepping, (v) the handling of csc θ terms, and (vi) the inclusion of azimuthal asymmetries must be considered. This work uses a split-operator formalism and a FSHT to present the first propagator to simultaneously overcome all six problems. As such, this propagator exhibits a general solution to the m-mixing problem, which has hampered the studies of systems with azimuthally asymmetric potentials.

We think that this propagator will be especially useful in several applications. First, the obviation of kinetic and potential matrix elements makes this propagator ideal for angular systems with numerical potentials. Such cases have recently been reported in studies of molecular alignment with surface-adsorbed molecules.[21] Second, imaginary time steps can be used with this propagator to easily diagonalize angular Hamiltonians with azimuthal asymmetries and/or numerical potentials. Third, we expect the incorporation of radial variables into this technique to be straightforward since they can be accelerated by the FFT.[7] Finally, we note that similar fast transforms for various canonical special functions have also been reported,[22] and can be combined with the split-operator formalism to yield efficient propagators for large classes of chemical problems.

ACKNOWLEDGMENTS

We are grateful to Dr. Jeff R. Hammond and Dr. Thorsten Hansen for interesting conversations and to the NSF Chemistry Division (Grant No. CHE-0616927) for their generous support. M.G.R. thanks the DoE Computational Science Graduate Fellowship Program (Grant No. DE-FG02-97ER25308) for a graduate fellowship.

[1] R. Kosloff, J. Phys. Chem. **92**, 2087 (1988).
[2] D. Lauvergnat, S. Blasco, X. Chapuisat, and A. Nauts, J. Chem. Phys. **126**, 204103 (2007).
[3] There are three factors limiting the size of Δt: (i) The propagator needs to remain accurate to second order. Higher-order split-operator schemes usually sacrifice unitarity, time reversibility, or both (Refs. 23 and 24). (ii) $\hat{\mathcal{V}}(t)$ needs to be approximately constant over the time step. (iii) $\max\{|\tilde{T}\Delta t/(2\hbar)|,|\tilde{V}(t+\Delta t/2)\Delta t/\hbar|\}\ll 2\pi$, where $\tilde{T}$ is the largest eigenvalue (in magnitude) of $\hat{T}$ whose corresponding eigenstate has non-negligible population, and similarly for $\tilde{V}(t+\Delta t/2)$.
[4] S. Egner and M. Püschel, IEEE Trans. Signal Process. **49**, 1992 (2001).
[5] M. D. Feit, J. A. Fleck, Jr., and A. Steiger, J. Comput. Phys. **47**, 412 (1982).
[6] M. D. Feit and J. A. Fleck, Jr., J. Chem. Phys. **78**, 301 (1983).
[7] M. D. Feit and J. A. Fleck, Jr., J. Chem. Phys. **80**, 2578 (1984).
[8] M. R. Hermann and J. A. Fleck, Jr., Phys. Rev. A **38**, 6000 (1988).
[9] T. K. Kjeldsen, L. A. A. Nikolopoulos, and L. B. Madsen, Phys. Rev. A **75**, 063427 (2007).
[10] C. E. Dateo and H. Metiu, J. Chem. Phys. **95**, 7392 (1991).
[11] G. C. Corey and D. Lemoine, J. Chem. Phys. **97**, 4115 (1992).
[12] M. Tygert, J. Comput. Phys. **227**, 4260 (2008).
[13] See, e.g., P. G. Martinsson and V. Rokhlin, SIAM J. Sci. Comput. (USA) **29**, 1160 (2007).

[14] M. Gu and S. C. Eisenstat, SIAM J. Matrix Anal. Appl. **16**, 172 (1995).
[15] The notation used in this work is similar to that of Ref. 12; however, some changes have been made in an attempt to increase clarity.
[16] A. Glaser, X. Liu, and V. Rokhlin, SIAM J. Sci. Comput. (USA) **29**, 1420 (2007).
[17] S. D. Cohen and A. C. Hindmarsh, Comput. Phys. **10**, 138 (1996).
[18] M. Frigo and S. G. Johnson, Proc. IEEE **93**, 216 (2005).
[19] Because the FMM is only exact in the limit of an infinite sum (arbitrary accuracy), the FSHT is also approximate but arbitrarily accurate. Our claim of unitarity should be interpreted as numerical unitarity within the specified tolerance.
[20] T. Seideman and E. Hamilton, Adv. At., Mol., Opt. Phys. **52**, 289 (2006).
[21] M. G. Reuter, M. Sukharev, and T. Seideman, Phys. Rev. Lett. **101**, 208303 (2008).
[22] M. Tygert, "Recurrence relations and fast algorithms," Department of Computer Science, Yale University Technical Report No. 1343, 2005.
[23] A. Bandrauk and H. Shen, Chem. Phys. Lett. **176**, 428 (1991).
[24] M. Suzuki, J. Math. Phys. **32**, 400 (1991).